# BUCKLING LOAD OPTIMIZATION OF THERMALLY STIFFENED PLATES WORKING ON TEMPERATURE RANGE WITH FINITE ELEMENTS

**Rodolfo Mazutti Meleiro, rodomaz@yahoo.com**
**José Antonio Hernandes, hernandes@ita.br**
Instituto Tecnológico de Aeronáutica – ITA São José dos Campos – SP, CEP 12228-900, Brazil

**Abstract.** *The buckling load of thermally stiffened laminated plates is directly dependent on the stiffness distribution over the plate. When using variable thickness within the plate the thermal residual stress can be used to increase the buckling load, although it can also decrease this load. So, in order to take the maximum advantage of residual stress it is necessary to optimize the stiffness distribution over the plate in such a way to increase the critical buckling load. This new improved laminate in practical applications will not be subjected to only one constant temperature, in fact for aeronautical structural components the typical working temperature is from –54ºC up to 80ºC. An usual optimization of laminated plates considers only one constant working temperature, but the final configuration may not be good for other temperatures, causing the component to buckle. Looking at the problem of working temperature range this paper studies the optimization of laminated plates working in a temperature range, optimizing the critical load considering the full range of temperature. For this study the objective function will be the buckling load maximized with respect to the layer's heights, using a FEM model.*

***Keywords**: buckling, optimization, laminated plates, thermal stiffness, finite elements*

## 1. INTRODUCTION

Laminated plates subjected to thermal differences can show thermal residual stress, depending basically on its geometry. In symmetrical plates residual stresses appears only if the plate is reinforced or constrained. Although it may feel that residual stress means a decrease in the plate buckling load, this is not always true. As a matter of fact, if reinforces are correctly designed an improvement in the critical load of the plate may occur (Almeida and Hansen, 1997). For this to happen the reinforce design need to take advantage of the residual stress distribution, which is a function of the temperature.

When a laminated plate works within a range of temperature, which is a more realistic situation, but is optimized for a certain fixed temperature, it may show a lower critical buckling load in another temperature. To avoid this failure in a component we may optimize the reinforcement considering the full temperature range, which will give us an optimal design for the full working temperature range.

This structural synthesis will be performed with a quadratic triangular plate finite element based on Reissner-Mindlin theory, proposed by Sze *et al.* (1997) and which has its formulation described in detail by Lucena Neto *et al.* (2001), where also its capability was enhanced to deal with membrane behavior, as a flat shell finite element .

## 2. FORMULATION AND RESULTS

### 2.1. AST6 finite element

Sze *et al.* (1997) proposed the AST6, a six node triangular element (Figure 1) based on Reissner-Mindlin theory for bending of plates. This element uses quadratic interpolation for bending degrees of freedom (DOF) and linear interpolation for out of plane shear strain. Lucena Neto *et al.* (2001) formulated the element explicitly, i.e., using analytical integration and added membrane DOF to it.

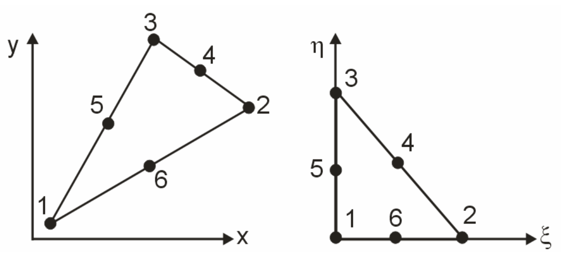


Figure 1. AST6 in global coordinates and local coordinates

To solve the buckling problem we will consider the pre-buckling stress state. Immediately before the buckling of the plate acting stresses are due to a loading identical to the critical load. In order to determine this stress state two linear independent static stress analyses must be done: one for thermal loading and another for mechanical loading.

Knowing the stress state we can compute the geometric stiffness matrices associated to each loading and then finally find the solution of the resulting eigenvalue problem.

Details in the formulation of laminated plates and the linear finite element will be omitted here, but the formulation of the geometric stiffness matrix for the AST6 will be shortly explained. The considered geometric stiffness formulation will be inconsistent, which means that the interpolation functions used to generate it are different from the ones used for the linear stiffness. In this case quadratic interpolation functions are used for all the terms in the geometric stiffness. This is done because the mesh locking effect does not occur with the non-linear deformation terms that appear in the geometric stiffness matrix. The full deduction of this matrix can be found at Meleiro (2006), which leads to:

$$[K_G] = \iint_A \left( [NN]^T [\Psi][NN] \right) dxdy \tag{1}$$

Where *$[K_g]$* is the geometric stiffness matrix, *$[NN]$* and *$[\Psi]$* are:

$$[NN] = \left[ [N_1] \quad [N_2] \quad [N_3] \quad [N_4] \quad [N_5] \quad [N_6] \right] \tag{2}$$

$$[N_i]^T = \begin{bmatrix} n_{i'x} & n_{i'y} & 0 & 0 & 0 & 0 & 0 & 0 & 0 & 0 & 0 & 0 \\ 0 & 0 & n_{i'x} & n_{i'y} & 0 & 0 & 0 & 0 & 0 & 0 & 0 & 0 \\ 0 & 0 & 0 & 0 & n_{i'x} & n_{i'y} & 0 & 0 & 0 & 0 & 0 & 0 \\ 0 & 0 & 0 & 0 & 0 & 0 & 0 & 0 & -n_{i'x} & -n_{i'y} & 0 & -n_i \\ 0 & 0 & 0 & 0 & 0 & 0 & n_{i'x} & n_{i'y} & 0 & 0 & n_i & 0 \end{bmatrix} \tag{3}$$

$$[\Psi] = \begin{bmatrix} N_{xx} & N_{xy} & 0 & 0 & 0 & 0 & M_{xx} & M_{xy} & 0 & 0 & Q_x & 0 \\ N_{xy} & N_{yy} & 0 & 0 & 0 & 0 & M_{xy} & M_{yy} & 0 & 0 & Q_x & 0 \\ 0 & 0 & N_{xx} & N_{xy} & 0 & 0 & 0 & 0 & M_{xx} & M_{xy} & 0 & Q_y \\ 0 & 0 & N_{xy} & N_{yy} & 0 & 0 & 0 & 0 & M_{xy} & M_{yy} & 0 & Q_y \\ 0 & 0 & 0 & 0 & N_{xx} & N_{xy} & 0 & 0 & 0 & 0 & 0 & 0 \\ 0 & 0 & 0 & 0 & N_{xy} & N_{yy} & 0 & 0 & 0 & 0 & 0 & 0 \\ M_{xx} & M_{xy} & 0 & 0 & 0 & 0 & L_{xx} & L_{xy} & 0 & 0 & T_x & 0 \\ M_{xy} & M_{yy} & 0 & 0 & 0 & 0 & L_{xy} & L_{yy} & 0 & 0 & T_y & 0 \\ 0 & 0 & M_{xx} & M_{xy} & 0 & 0 & 0 & 0 & L_{xx} & L_{xy} & 0 & T_x \\ 0 & 0 & M_{xy} & M_{yy} & 0 & 0 & 0 & 0 & L_{xy} & L_{yy} & 0 & T_y \\ Q_x & Q_x & 0 & 0 & 0 & 0 & T_x & T_y & 0 & 0 & 0 & 0 \\ 0 & 0 & Q_y & Q_y & 0 & 0 & 0 & 0 & T_x & T_y & 0 & 0 \end{bmatrix} \tag{4}$$

In Eq.(3) $n_i$ are the element displacement interpolation functions. The terms $N_{ij}$, $M_{ij}$, $Q_{ij}$, $L_{ij}$, $Q_i$ and $T_i$ are stress resultants, defined for mechanical loads as:

$$\begin{Bmatrix} \{N\} \\ \{M\} \\ \{L\} \end{Bmatrix} = \begin{bmatrix} [A] & [B] \\ [B] & [D] \\ [D] & [E] \end{bmatrix} \begin{Bmatrix} \{\varepsilon_m\} \\ \{\kappa\} \end{Bmatrix} \qquad \begin{Bmatrix} \{Q\} \\ \{T\} \end{Bmatrix} = \begin{bmatrix} [G] \\ [F] \end{bmatrix} \{\gamma\} \tag{5}$$

Thermal residual stresses (subscript *R*) are calculated by the difference between the free thermal stress (subscript *T*) and the resulting stress acting on the plate (no subscript).

$$\begin{Bmatrix} \{N_R\} \\ \{M_R\} \end{Bmatrix} = \begin{Bmatrix} \{N\} \\ \{M\} \end{Bmatrix} - \begin{Bmatrix} \{N_T\} \\ \{M_T\} \end{Bmatrix} \qquad \begin{Bmatrix} \{L_R\} \\ \{Q_R\} \\ \{T_R\} \end{Bmatrix} = \begin{Bmatrix} \{L\} \\ \{Q\} \\ \{T\} \end{Bmatrix} \tag{6}$$

$$\left(\{N_T\},\{M_T\}\right) = \sum_{k=1}^{N} \int_{z_k}^{z_{k+1}} [Q]\{\alpha\}\Delta T(1,z)\,dz \tag{7}$$

### 2.2. Buckling problem definition

The theory of buckling deals with conditions under which equilibrium ceases to be stable. A structure is said to be buckled when it loses stability (Reddy, 1997).

Buckling of laminated composite plates can happen caused basically by three types of loads: compression in fiber direction, compression normal to fiber direction (in plate plane) and by shear (also in plate plane). Any of these loads or combination of them will have a critical value, which is the load for which the plate loses stability and become buckled.

To calculate the critical load we have the following eigenproblem with two geometric stiffness matrixes, one due to the mechanical load and another one due to the thermal residual stress (subscript *R*):

$$\left([K] + \left[K_{gR}\right] + \lambda_c \left[K_g\right]\right)\{\phi\} = \{0\} \tag{8}$$

The critical buckling load factor $\lambda_c$ applies to the mechanical loads, which cause plate instability. This factor is the quantity we want to increase, so it will be the objective function of our design optimization of plate reinforcements.

### 2.3. Reinforcements design optimization

Optimization theory deals with finding the minimum or maximum value of a given objective function, restrained or not by constraint functions. In this problem we will apply reinforcements to the composite plate as extra layers in predefined directions, forming different patterns over the laminate. The design variables will be the heights of the reinforcement layers. The optimization problem is:

$$\max \lambda_c\left(\{X\}\right)$$
$$s.t.: \begin{cases} g_m\left(\{X\}\right) = \dfrac{m\left(\{X\}\right)}{m_{\max}} - 1 \le 0 \\ g_i\left(\{X\}\right) = z_i - z_{i+1} \le 0, i = 1,\ldots,n_c \\ z_i^L \le z_i \le z_i^U, i = 1,\ldots,n_c \end{cases} \tag{9}$$

The objective function, i.e., the critical buckling factor, is under two types of constraints. The first one states that the mass of the plate can not be higher than $m_{max}$, which in our study cases will be the initial mass of the plate, so that plate buckling load will be improved without adding any mass to it. The second constraints limit the heights of subsequent layers such that no penetration between layers may happen.

To solve an optimization problem we need to constantly modify the design variables and calculate the objective and constrain functions. These calculations may have a high computational cost, because here these functions are associated to the solution of many finite element eigenvalue problems. In order to decrease the computational cost the RQA approximation technique will be used (Canfield, 1988). This consists in solving the full finite element model to determine the critical buckling loads and buckling modes and also the derivates of modal strain and kinetic energies which respect to the design variables, and then use this information to create an approximation of the critical buckling load. The critical load factor is given in terms of the Rayleigh quotient as:

$$\lambda_c = \frac{U}{T} = \frac{\{\phi\}^T \left([K] + \left[K_{gT}\right]\right)\{\phi\}}{-\{\phi\}^T \left[K_g\right]\{\phi\}} \tag{10}$$

In Eq.(10) $U$ is the modal strain energy and $T$ is the modal kinetic energy. The RQA approximation for $\lambda_c$ is given by

$$\tilde{\lambda}(\{X\}) = \frac{U(\{X_0\}) + \sum_{k=1}^{NVA} \left( \frac{dU(\{X_0\})}{dy_k}(y_k - y_{0k}) \right)}{T(\{X_0\}) + \sum_{k=1}^{NVA} \left( \frac{dT(\{X_0\})}{dy_k}(y_k - y_{0k}) \right)} \tag{11}$$

The temperature range will be discretized in 5 points, such that the optimization problem of Eq. 9 becomes one of maximization of the minimum eigenvalue:

$$\max\ \min\left(\lambda_{ck}(\{X\})\right)$$
$$s.t.: \begin{cases} g_m(\{X\}) = \dfrac{m(\{X\})}{m_{\max}} - 1 \le 0 \\ g_i(\{X\}) = z_i - z_{i+1} \le 0, i = 1,\ldots,n_c \\ z_i^L \le z_i \le z_i^U, i = 1,\ldots,n_c \end{cases} \tag{12}$$

In Eq.(12) $\lambda_{ck}$ is the critical buckling load factor for one of the temperatures in which the range is discretized.

### 2.4. Study Case 1 – Longitudinal reinforcement

The first study case will be a plate with eight reinforcements in along its longitudinal direction, symmetric with respect to the plate centerline and also to the plate midsurface. All regions have the same width, and because of the symmetry only 4 different regions are defined. The reinforcements are applied over a constant base plate, and the heights of the pair of layers defining each reinforcement are design variables, therefore resulting in a total of 8 design variables ($h_1$ to $h_8$). The plate geometry and dimensions are shown in Fig. 2 along with the design variables ($xz$ plane view).

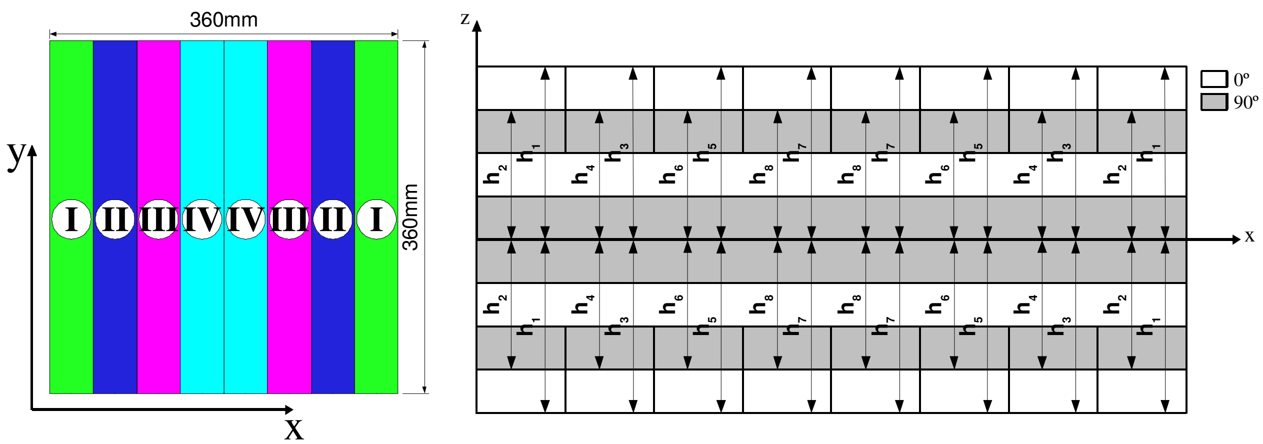


Figure 2. Geometry of plate with longitudinal reinforcements

The initial value for all layers thickness is 0.15mm, which is constant for the base plate. Typical fiber glass material properties shown in Tab.1 are used with the laminate sequence shown Tab. 2.

Table 1. Typical fiber glass properties

| Properties | Value |
|---|---|
| Longitudinal elastic modulus, $E_1$ | 154.5 GPa |
| Transverse elastic modulus, $E_2$ | 11.13 GPa |
| In plane poisson ratio, $n_{12}$ | 0.304 |
| Transverse shear modulus, $G_{23}$ | 3.36 GPa |
| Transverse shear modulus, $G_{13}$ | 6.98 GPa |
| In plane shear modulus, $G_{12}$ | 6.98 GPa |
| Longitudinal thermal expansion coefficient, $a_1$ | -0.17 X $10^{-6}$/ºC |
| Transverse thermal expansion coefficient, $a_2$ | 23.1 X $10^{-6}$/ºC |

Table 2. Laminate sequence for case 1

| Region | Lamiate sequence |
|---|---|
| I | $[0,90,0,90]_s$ |
| II | $[0,90,0,90]_s$ |
| III | $[0,90,0,90]_s$ |
| IV | $[0,90,0,90]_s$ |

This plate is simple supported on all four edges, with lower-left corner constrained in *x*, *y* and *z* directions. The lower horizontal edge is restrained in the *y direction*, while the upper horizontal edge has a -0.0036mm imposed displacement (*y direction)*, such that the plate is compressed in this direction. The working temperature range for this case is between -100ºC and -200ºC.

The original symmetrical plate with its four regions initially equal, has a constant critical buckling load because no thermal residual stress are present prior to plate optimization. As the optimization starts it runs towards a configuration where thermal residual stress are induced in a such a way to contribute to the increase of the buckling load. The optimal final configuration obtained has the critical buckling load versus temperature curve shown in Fig. 3, which is normalized with respect to the initial plate buckling load. It can be observed that a increase of more than 150% in the buckling load was possible. The optimum values of the design variables are presented in Tab. 3, corresponding to the *xz* view of the plate of Fig. 4. It can be seen that the optimal plate became thicker in the central region where the reinforcements consist of layers oriented at $0°$ and thinner at the edges with $0°$ and $90°$ layers.

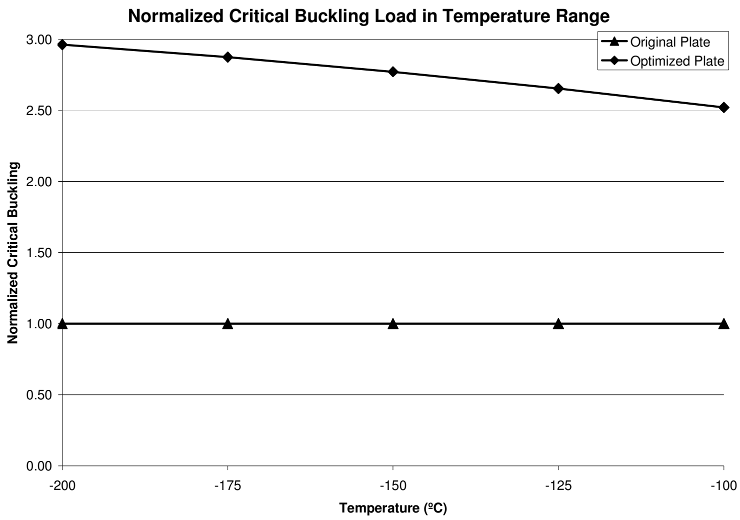


Figure 3. Case 1 normalized critical buckling load versus temperature

Table 3. Case 1 design variables final values (mm)

| $h_1$ | $h_2$ | $h_3$ | $h_4$ | $h_5$ | $h_6$ | $h_7$ | $h_8$ |
|---|---|---|---|---|---|---|---|
| 0.483 | 0.483 | 0.519 | 0.300 | 0.669 | 0.300 | 0.729 | 0.300 |

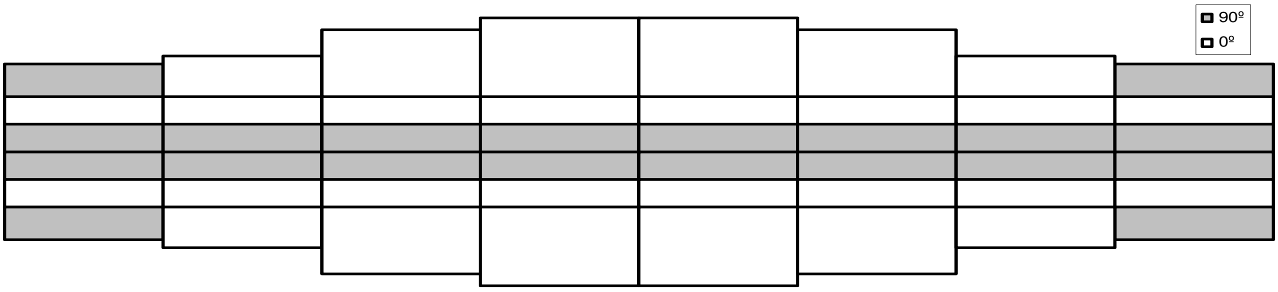


Figure 4. Optimized plate *xz* view

From Fig. 3 one can see that the buckling load variation with the temperature is smooth, almost linear. In fact the critical mode was observed to be nearly the same for all the temperature range, and so from Eq. 10 it can be seen that $\lambda_c$ becomes directly dependent on the thermal residual geometric stiffness matrix , which is directly proportional to temperature. The curve isn't linear because the critical mode in fact will have its shape slightly changed in the five discretization temperatures used.

**2.4. Study Case 2 – Frame shape reinforcement**

For this case a plate with same size and material from the previous test is considered. Also the base plate is still the same, but now its height is also a design variable. The main difference will be the reinforcement shape, which is now a frame as shown in Fig. 5, with cut views AA and BB in Fig. 6 showing the design variables ($h_1$ to $h_6$).

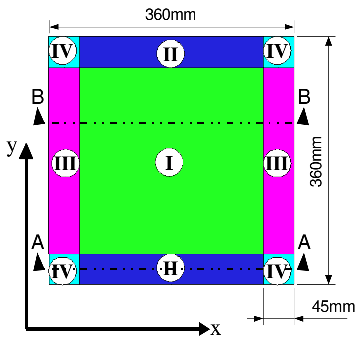


Figure 5. Optimized plate *xz* view

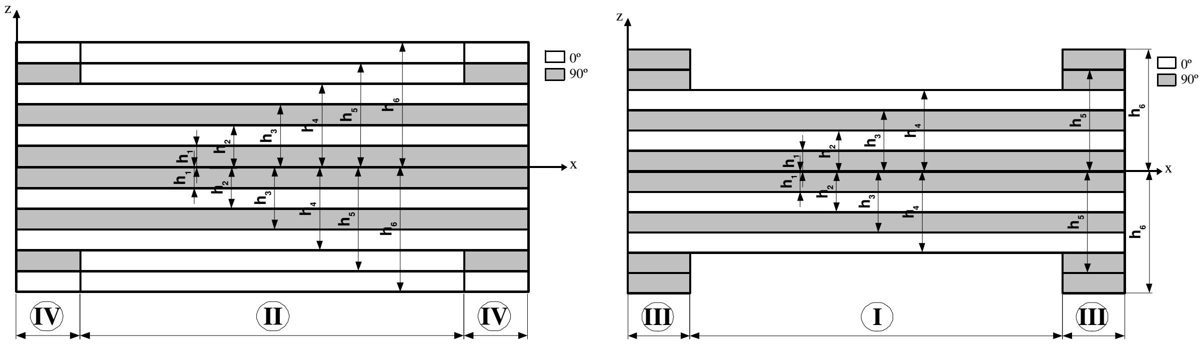


Figure 6. AA and BB cut views from Fig. 5

The laminate sequence for each region is in Tab. 4, and again the initial thickness for each layer is 0.15mm. In this case the plate will be optimized to support two different load conditions. For both cases all edges will be simple-supported with the lower-left corner restrained in *x*, *y* and *z* directions. The first load is a biaxial compression, applied with the lower edge constrained in *y* direction while the upper edge has -0.0002mm displacement in *y* direction, and the left edge constrained in *x*direction with the right edge having -0.0002mm in the *x* direction. The second load condition is a shear load case, with the vertical edges angularly deformed of $\Delta$=1°, keeping the plate perimeter constant and the opposite plate edges parallel (Fig. 7). The small biaxial displacement is is used to force the biaxial buckling load to be equal the shear buckling load in the initial model, so both load cases are critical.

Table 4. Laminate sequence for case 2

| Region | Lamiate sequence |
|---|---|
| I | $[0,90,0,90]_s$ |
| II | $[0,0,0,90,0,90]_s$ |
| III | $[90,90,0,90,0,90]_s$ |
| IV | $[0,90,0,90,0,90]_s$ |

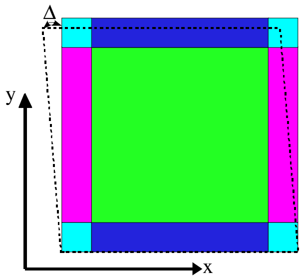


Figure 7. Applied shear deformation

The graph in Fig. 8 shows the critical buckling load of the optimized plate under two load conditions in the temperature range considered, normalized with respect to the the minimum initial plate buckling load, within the temperature range. It can be observed that a significant increase of 169% in the buckling load factor could be obtained. The optimum values of the design variables values are in Tab. 5, from where with the help of Fig. 6, it can be seen that the reinforcements had a increase of thickness with respect to the initial configuration and the fourth initial layer was eliminated. .

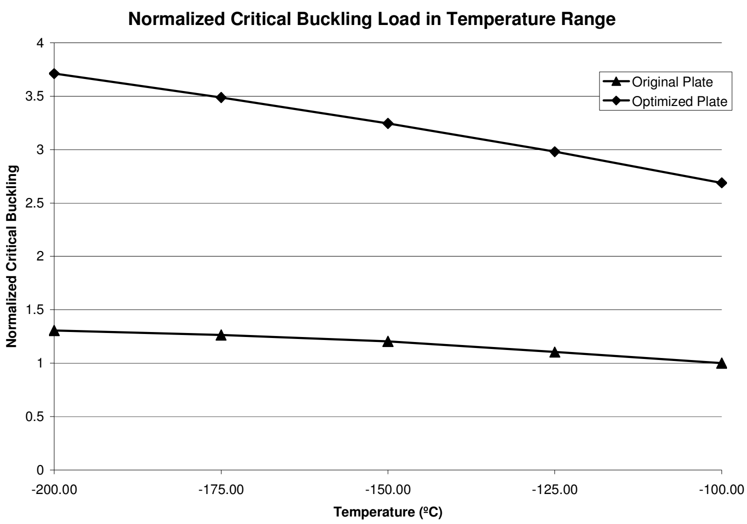


Figure 8. Case 2 normalized critical buckling load versus temperature

Table 5. Case 2 design variables final values (mm)

| $h_1$ | $h_2$ | $h_3$ | $h_4$ | $h_5$ | $h_6$ |
|---|---|---|---|---|---|
| 0.207 | 0.207 | 0.315 | 0.315 | 0.938 | 1.267 |

From Fig. 7, firstly it should be noticed that the initial plate critical buckling load is not constant as in case 1. This is because the initial plate configuration already possessing frame reinforcements has also initial residual thermal stress. Again, even with the two applied load cases, the optimal plate configuration has an almost linear behavior of the critical load with temperature. This seems to be the tendency of the composite plate optimization with the types of reinforcements used here.

### 2.4. Conclusions

The use of appropriate techniques of structural optimization for the design of laminated composite plates under residual thermal stress, working in a given temperature range produced, with very modest computational resources, optimal solutions showing a high increase of plate resistance to buckling can be achieved. Also, from the studied cases it was observed a nice behavior of the optimization convergence, with no difficulties present, specially with respect to the shifting of fundamental modes, which may be expected as a source of difficulty in composite plate design optimization. As a matter of fact the optimal designs obtained are in such a way that the critical modes are very similar at the different temperatures along the entire temperature range.. This means that the critical load variation is a smooth function of the temperature range, tending to linearity, which means that the optimization could be done for the worse temperature of the interval. For instance, in cases 1 and 2, this would mean to optimize the critical load for $\Delta T$=-100º, with a new constrain forcing this to be the lowest load within the range, i.e., $\delta\lambda_c/\delta T<0$.

## 3. REFERENCES

Almeida, S. F. M., Hansen, J. S.,1997, "Enhanced Elastic Buckling Loads of Composite Plates With Tailored Thermal Residual Stresses", Journal of Applied Mechanics, Vol. 64, pp. 772-780

Canfield, Robert A, 1988, "An Approximation Function for Frequency Constrained Structural Optimization," Second NASA/Air Force Symposium on Recent Advances in Multidisciplinary Analysis and Optimization, NASA, Hampton, VA, Sept 28-30, pp. 937-953.

Lucena Neto, E., Goto, S. T., e Kataoka Filho, M., 2001, "Um Elemento Triangular Eficiente para Placas Laminadas", Campinas, Brazil, 22nd Iberian Latin-American Congress on Computational Methods in Engineering, pp. 18

Meleiro, R. M., 2006, "Síntese de Laminados com o Elemento AST6 Operando em Faixa de Temperatura", Master Degree Thesis, São José dos Campos:ITA

Reddy, J. N.,1997, "Mechanics of Laminated Composite Plates: Theory and Analysis", Ed. CRC Press

Sze, K. Y., Zhu, D., Chen, D.,1997, "Quadratic Triangular $C^0$ Plate Bending Element", International Journal for Numerical Methods in Engineering, Vol. 40, pp. 937-951

## 4. RESPONSIBILITY NOTICE